

1  
2  
3  
4  
5  
6  
7  
8  
9  
10  
11  
12  
13  
14  
15  
16  
17  
18  
19  
20  
21  
22  
23  
24  
25  
26

Drug combination sensitivity scoring facilitates the discovery of synergistic and efficacious drug combinations in cancer

Alina Malyutina<sup>1</sup>, Muntasir Mamun Majumder<sup>1</sup>, Wenyu Wang<sup>1</sup>, Alberto Pessia<sup>1</sup>, Caroline A. Heckman<sup>1</sup>, Jing Tang<sup>1,2\*</sup>

<sup>1</sup>Institute for Molecular Medicine Finland (FIMM), Helsinki Institute of Life Science, University of Helsinki, Helsinki, Finland

<sup>2</sup>Department of Mathematics and Statistics, University of Turku, Turku, Finland

\* Corresponding author

E-mail: [jing.tang@helsinki.fi](mailto:jing.tang@helsinki.fi) (JT)

## 27 **Abstract**

28 High-throughput drug sensitivity screening has been utilized for facilitating the discovery of drug  
29 combinations in cancer. Many existing studies adopted a dose-response matrix design, aiming for  
30 the characterization of drug combination sensitivity and synergy. However, there is lack of  
31 consensus on the definition of sensitivity and synergy, leading to the use of different mathematical  
32 models that do not necessarily agree with each other. We proposed a cross design to enable a more  
33 cost-effective testing of sensitivity and synergy for a drug pair. We developed a drug combination  
34 sensitivity score (CSS) to summarize the drug combination dose-response curves. Using a high-  
35 throughput drug combination dataset, we showed that the CSS is highly reproducible among the  
36 replicates. With machine learning approaches such as Elastic Net, Random Forests and Support  
37 Vector Machines, the CSS can also be predicted with high accuracy. Furthermore, we defined a  
38 synergy score based on the difference between the drug combination and the single drug dose-  
39 response curves. We showed that the CSS-based synergy score is able to detect true synergistic and  
40 antagonistic drug combinations. The cross drug combination design coupled with the CSS scoring  
41 facilitated the evaluation of drug combination sensitivity and synergy using the same scale, with  
42 minimal experimental material that is required. Our approach could be utilized as an efficient  
43 pipeline for improving the discovery rate in high-throughput drug combination screening. The R  
44 scripts for calculating and predicting CSS are available at <https://github.com/amalyutina/CSS>.

45

## 46 **Author summary**

47 Being a complex disease, cancer is one of the main death causes worldwide. Although new  
48 treatment strategies have been achieved with cancers, they still have limited efficacy. Even when  
49 there is an initial treatment response, cancer cells can develop drug resistance thus cause disease

50 recurrence. To achieve more effective and safe therapies to treat cancer, patients critically need  
51 multi-targeted drug combinations that will kill cancer cells at reduced dosages and thereby avoid  
52 side effects that are often associated with the standard treatment. However, the increasing number  
53 of possible drug combinations makes a pure experimental approach unfeasible, even with  
54 automated drug screening instruments. Therefore, we have proposed a new experimental set up to  
55 get the drug combination sensitivity data cost-efficiently and developed a score to quantify the  
56 efficiency of the drug combination, called drug combination sensitivity score (CSS). Using public  
57 datasets, we have shown that the CSS robustness and its highly predictive nature with an accuracy  
58 comparable to the experimental replicates. We have also defined a CSS-based synergy score as a  
59 metric of drug interaction and justified its relevance. Thus, we expect the proposed computational  
60 techniques to be easily applicable and beneficial in the field of drug combination discovery.

61

## 62 **Introduction**

63 Despite the great advances in the understanding of cancer, there remains a major gap  
64 between the vast knowledge of molecular biology and effective anti-cancer treatments. Next  
65 generation sequencing has revealed the intrinsic heterogeneity in cancer survival pathways, which  
66 partly explains why patients respond differently to the same therapy [1]. To reach effective and  
67 durable clinical responses, cancer patients who become resistant to standard treatments need  
68 multi-targeted drug combinations, which shall effectively inhibit the cancer cells and block the  
69 emergence of drug resistance [2-4].

70 In order to predict novel drug combinations, high-throughput drug screening has been  
71 applied on a large variety of cancer cell lines and more recently on patient-derived cancer samples  
72 [5-6]. Ideally, a promising drug combination should achieve the therapeutic efficacy at reduced

73 dosages, and therefore also minimize the toxicity and other side effects associated with high doses  
74 of single drugs [7-8]. Therefore, both the sensitivity and synergy of a drug combination need to be  
75 considered when evaluating the high-throughput screening results for further validation [9].

76 Many high-throughput drug combination screens combine two drugs at a full matrix of  
77 multiple doses, for which the cell viability or growth inhibition effects are measured [10-11]. The  
78 drug combinations are usually ranked based on the degree of synergy, such that the drug  
79 combinations that produce higher growth inhibition effects compared to the single drugs will be  
80 prioritized. However, there have been multiple methods to score drug synergy, each of which relies  
81 on a different mathematical model that do not fully agree with each other [12]. The lack of  
82 consensus on the choice of synergy scoring methods may partly explain the difficulty to validate  
83 drug combination discoveries in a high-throughput setting [13]. On the other hand, focusing only on  
84 synergy but not on sensitivity may produce false positive drug combinations that do not necessarily  
85 reach therapeutic efficacy, despite being synergistic [14]. However, unlike the sensitivity of single  
86 drugs which can be directly derived from dose-response curves [15], the sensitivity of a drug  
87 combination remains largely undefined, as the same sensitivity can be achieved using different dose  
88 combinations. Furthermore, there is a lack of scoring approaches to fully capture the synergy and  
89 sensitivity simultaneously.

90 On the other hand, the dose-response matrix utilizes a full factorial design to test multiple  
91 dose combinations, and thus demands a relatively large amount of cancer cells. For patient-derived  
92 cancer samples which are typically rare and restricted in volume, the full dose-response matrix  
93 design may be infeasible for testing even a minimal number drug combinations. Furthermore,  
94 cancer samples of different genetic profiles are known to respond differently to the same drug  
95 combination. With the limited amount of drug combinations as the training data, it becomes a

96 daunting task for any machine learning approach to navigate the combinatorial space to pinpoint  
97 the most promising drug combinations that are specific for individual cancer samples [16].

98 To overcome these challenges, we proposed a cost-effective experimental and  
99 computational procedure to facilitate the prediction of drug combination synergy and sensitivity.  
100 We utilized an experimental design where two drugs are crossed at their IC<sub>50</sub> concentrations, and  
101 either drug is allowed to span over multiple doses while the concentration of the other drug is fixed.  
102 The resulting dose-response curves are utilized to defined a drug combination sensitivity score  
103 (CSS). Using a large scale of drug combination study, referred to as the O'Neil data [17], we showed  
104 that the CSS is highly reproducible, suggesting its robustness as a metric for characterizing drug  
105 combination responses. Furthermore, we found that the CSS can be predicted at high accuracy using  
106 chemical and pharmacological features of the drug combinations. Based on the difference between  
107 the observed and expected CSS values, a drug synergy score can be determined straightforwardly.  
108 We showed that such a CSS-based synergy score can also detect the true synergistic and  
109 antagonistic drug combinations with high accuracy. Compared to the dose-response matrix design,  
110 the cross design requires minimal amount of experimental materials, while it still maintains a  
111 sufficient level of accuracy for capturing both synergy and sensitivity simultaneously. We foresee  
112 that such an experimental design and its CSS scoring would facilitate the standardization of drug  
113 combination analysis that is currently lacking in functional chemical screening, and would allow for  
114 the scale up of drug combination testing eventually for personalized medicine.

115

## 116 **Results**

### 117 **CSS values are highly reproducible and robust**

118 We applied the CSS scoring on the O'Neil drug combination data, which consists of 22,737  
119 drug combinations for 39 cancer cells [17]. We found that the CSS<sub>1</sub> and CSS<sub>2</sub> values calculated using

120 either drug fixed at its  $IC_{50}$  concentration are highly correlated (Pearson correlation = 0.82, p-value  
121 =  $2 \times 10^{-16}$ ; Fig 1A). Both  $CSS_1$  and  $CSS_2$  values ranged from 0 to 50, with a marginal absolute difference  
122 of 5.62 (Fig 1B). Such a high level of consistency holds true for all the 39 cancer cell lines and the  
123 majority of the 38 unique drugs, suggesting the robustness of the CSS scoring method (Figs 1C and  
124 D, Fig S1). We also found a high correlation between the CSS value and those derived from single  
125 replicates (minimal correlation = 0.97, Table S3). In order to check whether the CSS values are within  
126 the range of the CSS replicates for each drug combination, we calculated the minimal and maximal  
127 values over the CSS replicates for each drug combination and plotted them together with CSS values  
128 over the standard deviation of the CSS replicates. For a better visualization, we applied a generalized  
129 additive model to smoothen the CSS lines and obtain 95% pointwise confidence interval around the  
130 mean (Fig S2). Only 4% of the drug combinations have the CSS values being out of the CSS replicate-  
131 based limits, however this can be explained by the higher variance over the replicates.

132 **Fig 1. Robustness and replicability of CSS.** (A) The correlation of  $CSS_1$  and  $CSS_2$  over all the drug  
133 combinations; (B) Density plot of the  $CSS_1$  and  $CSS_2$  distributions; (C) The correlation per cell line  
134 colored according to the tissue type; and (D) The correlation per drug colored according to the drug  
135 target class.

136 Notably, we found that drug combinations that involved bortezomib showed much lower  
137 correlation (0.26) between the  $CSS_1$  and  $CSS_2$  values compared to other drug combinations. Since  
138 the O'Neil data contains the replicates for single drug screening, we analyzed the coefficient of  
139 variation (CV) of the cell viability readout for each drug in the replicates. As expected, we found that  
140 bortezomib has the highest CV (0.28), suggesting a relative low quality of the drug sensitivity data  
141 involving this drug (Fig S3). Therefore, the lower correlation between the  $CSS_1$  and  $CSS_2$  for a drug  
142 combination may be attributed to a higher experimental variation, and thus were considered as low  
143 quality data points. For the subsequent analysis, we selected only those drug combinations that

144 have the absolute difference between  $CSS_1$  and  $CSS_2$  lower than 10, resulting in a total of 18,905  
145 drug combinations. After this filtering the correlation between  $CSS_1$  and  $CSS_2$  was further improved  
146 (Pearson correlation = 0.93, p-value =  $2 \times 10^{-16}$ ). Furthermore, the mean absolute difference between  
147  $CSS_1$  and  $CSS_2$  was 3.83, which became comparable to the variability determined from the technical  
148 replicates of  $CSS_1$  and  $CSS_2$  (2.92 and 3.06 respectively), suggesting that the difference between  $CSS_1$   
149 and  $CSS_2$  is similar to what is expected when repeating the experiment. Taken together,  $CSS_1$  and  
150  $CSS_2$  values are highly consistent and therefore supported their averaging as a summary for the drug  
151 combination sensitivity score.

## 152 **CSS can be predicted using machine learning approaches**

153         Given that the CSS is highly reproducible as a summary of the overall sensitivity of a drug  
154 combination, we explored whether CSS can be predicted using pharmacological and chemical  
155 information of the drugs. We considered a drug combination as a combination of its drugs target  
156 profiles as well as their chemical fingerprints, with which the machine learning approaches  
157 illustrated in the previous section can be optimized by exploring the feature space using the training  
158 data. We examined three major machine learning methods for predictions: Elastic Net, Random  
159 Forests and Support Vector Machines.

160         We found that all of these machine learning approaches worked reasonably well, with the  
161 Elastic Net consistently achieving the best performance, with the mean MAE of 4.01 which is  
162 comparable to that (2.07) of a technical replicate (Table 1). Note that in our cross-validation setting  
163 the drug combinations in the test data were not present in the training data, the machine learning  
164 methods were still able to predict the CSS values for new drug combinations by exploring the feature  
165 similarity in the drug targets and chemical fingerprints. The prediction performance thus validated  
166 our hypothesis that a drug combination can be considered as a combination of their drug target

167 profiles and chemical-structural properties, with which the CSS score can be predicted with high  
168 confidence using the state-of-the-art machine learning approaches.

169 **Table 1. The prediction performance for Elastic Net, Random Forests and Support Vector**  
170 **Machines, as compared to the upper limit when selecting randomly one technical replicate as the**  
171 **prediction.**

<i>Method</i>	<i>RMSE</i>	<i>R2</i>	<i>COR</i>	<i>MAE</i>
<i>Elastic Net</i>	5.20±1.11	0.80±0.06	0.90±0.03	4.01±0.86
<i>Random Forests</i>	6.30±1.18	0.71±0.07	0.85±0.04	4.75±0.9
<i>Support Vector Machines</i>	7.47±1.32	0.57±0.08	0.80±0.04	5.80±1.07
<i>Technical replicate</i>	2.87±0.59	0.93±0.04	0.97±0.02	2.07±0.45

172 All the values are mean+/-standard deviation.

173 Since both the drug target profiles and chemical fingerprints were considered as the drug  
174 combination features, we next evaluated their prediction performances separately using the Elastic  
175 Net method. For drug-target profiles we collected known targets that were experimentally validated  
176 as well as the additional secondary targets that were predicted with high confidence using the SEA  
177 method. For chemical fingerprints we used the MACCS fingerprint which contains 166 structural  
178 features [18]. As expected, when combining all the features the model achieved the best  
179 performance (Table 2). We found that in general drug target profiles were predictive of CSS,  
180 especially when including the experimentally validated targets. The predicted targets using the SEA  
181 method did not improve the prediction accuracy significantly, indicating that even though  
182 secondary drug target interactions may occur, most likely they have minor functional impact that  
183 may not lead to the changes in cancer cell viability and thus does not contribute to the prediction  
184 of CSS. On the other hand, we found that chemical fingerprints were less predictive of CSS compared  
185 to the drug-target profiles, suggesting that the use of MACCS might be suboptimal to capture the  
186 relevant structural information for predicting the drug combination sensitivity. However, as the



187 focus of this study was to show the validity of using machine learning methods to predict the CSS  
188 score, we decided to explore other chemical fingerprint features as a future step.

189 **Table 2. The prediction performances for drug-target features and chemical fingerprint features**  
190 **using Elastic Net.**

<i>Feature</i>	<i>RMSE</i>	<i>R2</i>	<i>COR</i>	<i>MAE</i>
<i>Validated targets</i>	5.66±1.27	0.77±0.07	0.88±0.04	4.26±0.95
<i>Validated + predicted targets</i>	5.70±1.22	0.76±0.06	0.87±0.04	4.34±0.95
<i>Fingerprints</i>	6.27±1.19	0.71±0.06	0.85±0.04	4.87±0.94
<i>Validated targets + fingerprints</i>	5.30±1.14	0.79±0.06	0.89±0.03	4.07±0.88
<i>All features</i>	5.20±1.11	0.80±0.06	0.90±0.03	4.01±0.86

191 All the values are mean+/-standard deviation.

192 We considered the regression coefficients that were determined in the Elastic Net model as  
193 an indication of their importance to contribute to the CSS prediction. We collected 67 features that  
194 have their absolute coefficients greater than 3 for at least one cell line. Unsupervised hierarchical  
195 clustering with the Manhattan metric was then applied to group the cell lines and the selected  
196 features (Fig 2). We found that certain drug target features were present with high coefficients  
197 across all the cell lines. For example, DNA topoisomerases including TOP1MT, TOP2A, TOP2B and  
198 TOP1 were selected, with an average coefficients of 8.2, 2.7, 2.6 and 1.0 separately. Despite the  
199 difference in the level of variable importance, all the DNA topoisomerases showed positive  
200 coefficients in 38 of 39 cell lines, suggesting that targeting DNA topoisomerases were associated  
201 with a higher CSS. DNA topoisomerases are known proteins which are essential for cell replication  
202 and metabolism [19]. Including a topoisomerase inhibitor can thus enhance the drug combination  
203 sensitivity in many cancer cell lines. On the other hand, the only cell line that showed negative

204 coefficients for TOP1MT was LNCAP (prostate cancer), which turned out to be the cell line that has  
205 the smallest average CSS scores for drug combinations involving the TOP1MT inhibitor (topotecan)  
206 (Fig S4).

207 **Fig. 2. The feature importance map by Elastic Net for each cell line.** Cell-line independent as well  
208 as cancer subtype-specific features can be identified by evaluating the regression coefficients of the  
209 Elastic Net model. Features such as TOP1MT, TOP1, TOP2A/B has shown consistently positive  
210 coefficients as compared to features such as AKT1/2/3 which showed cancer subtype specificity in  
211 breast cancer (indicated as arrows).

212 At the cell line level, we found that cell lines of the same tissue type did not necessarily  
213 cluster together, indicating their distinctive drug combination response profiles. However, we found  
214 that the breast cancer cell lines did form a major cluster including KPL1, ZR751, EFM192B, OCUBM  
215 and T47D, while the only outlier was MDAMB436. Indeed, MDAMB436 is the only triple negative  
216 breast cancer (TNBC) subtype, while the other cell lines are either ER positive (KPL1, ZR751 and  
217 T47D), or HER2 positive (EFM192B and OCUBM). It has been known that TNBC respond anticancer  
218 drugs differently from ER and HER2 positive breast cancers due to the distinctive disease  
219 mechanisms [20]. The features selected for the CSS prediction separated these two distinctive  
220 breast cancer subtypes, suggesting the validity of using CSS to cluster cancer of different subtypes.  
221 Furthermore, we found that AKT targets (AKT1/2/3) were among the top ones that showed higher  
222 importance in the non-TNBC group. A combination of an AKT inhibitor and TOP1MT inhibitor  
223 therefore can be suggested to treat non-TNBC but not necessarily for TNBC breast cancers. On the  
224 other hand, we found that CHEK1 and PARP3/4 targets were selected for MDAMB436 but not for  
225 non-TNBC group, suggesting that a combination of a CHEK inhibitor and PARP inhibitor might be  
226 tested for TNBC, but not for non-TNBC. The mechanisms of actions for the proposed drug  
227 combination may prove interesting for experimental validations. Taken together, the features that

228 were selected from the CSS prediction may help to pinpoint the underlying target interactions,  
229 which are of pivotal importance to identify the drug combination response biomarkers.

230

### 231 **The CSS-based synergy scores can predict the true synergy and antagonism**

232 Next, we defined the degree of drug synergy as the differences between the dose-response  
233 curves of a drug combination and its single drugs. We derived three variants of the CSS-based  
234 synergy score ( $S_{sum}$ ,  $S_{max}$ ,  $S_{mean}$ ) and compared them with the HSA, Bliss, Loewe and ZIP synergy  
235 scores that were determined using the full-dose response matrix. We evaluated whether the CSS-  
236 based synergy scores using the cross design can capture the ground truth. Although determined  
237 using only one row and one column from the dose-response matrix, all the CSS-based synergy scores  
238 managed to obtain a good correlation with the synergy scores based on the dose-response matrix  
239 design (Table 3).

240 **Table 3. Correlations of the CSS-based synergy scores with those derived using four reference**  
241 **models that were calculated using the full dose-response matrices.**

<i>Synergy Scores</i>	<i>HSA</i>	<i>Bliss</i>	<i>Loewe</i>	<i>ZIP</i>
$S_{sum}$	0.72	0.72	0.46	0.55
$S_{max}$	0.71	0.65	0.51	0.49
$S_{mean}$	0.65	0.63	0.41	0.44

242

243 We found that the CSS-based synergy scores correlated relatively well with the HSA and Bliss  
244 scores, while the correlation started to decrease when comparing to the Loewe and ZIP scores. Since  
245 all the synergy scoring models utilized different assumptions for the reference of no synergy, we  
246 therefore did not expect a perfect correlations in such pairwise comparisons. Of all the three  
247 variations of CSS-based synergy score, we found that  $S_{sum}$  showed the best correlation with those

248 determined using the full dose-response matrix. As  $S_{\text{sum}}$  considers the additive effect of single drug  
249 sensitivities as the expectation of no synergy, it thus can be considered a more conservative scoring  
250 method compared to  $S_{\text{max}}$  and  $S_{\text{mean}}$ , where the maximal and average effect of single drugs were  
251 considered as reference separately. To control the false discovery rate of detecting synergistic  
252 combinations, we therefore proposed  $S_{\text{sum}}$  as a more appropriate scoring method for the cross drug  
253 combination design.

254 Furthermore, we evaluated the predicting accuracy of the CSS-based synergy scores for true  
255 synergistic and antagonistic drug combinations. We applied a stringent criteria to determine the  
256 ground truth from the dose response matrix data, such that all the synergy scores (HSA, Bliss, Loewe  
257 and ZIP) must be higher than 5, or lower than -5, to be classified as a true synergistic or antagonistic  
258 drug combination, respectively. From the O'Neil data, we identified 3,716 true synergistic and 218  
259 true antagonistic drug combinations. We then asked the question of whether the CSS-based synergy  
260 scores that were determined using the cross design can predict the ground truth. We showed that  
261 the CSS-based synergy scores managed to achieve the area under the ROC curves of 0.997 ( $S_{\text{sum}}$ ),  
262 0.996 ( $S_{\text{max}}$ ) and 0.992 ( $S_{\text{mean}}$ ) to detect the true synergistic and antagonistic combinations correctly  
263 (Fig 3A). Note that in order to calculate the synergy score, only two vectors of the drug combination  
264 responses are needed, rather than the full dose-response matrix. Therefore, the CSS-based synergy  
265 score needs a substantially fewer measurements compared to the other well-established synergy  
266 scores. Still, the CSS-based synergy scores can predict the most synergistic and antagonistic drug  
267 combinations with high accuracy. On the other hand, the CSS-based synergy score and the CSS drug  
268 combination sensitivity score were using the same unit as the percentage of the actual drug  
269 response compared to the theoretical upper limit. Therefore, the synergy score can be interpreted  
270 as the extra benefit of combining two drugs that can achieve an effect closer to the upper limit. We  
271 summarized both CSS drug sensitivity scores and CSS-based synergy scores for all the drug

272 combinations as an S (sensitivity)-S (synergy) plot (Fig 3B; Table S4). By applying a threshold of the  
273 3<sup>rd</sup> quantiles for CSS and S, we can clearly identify the most promising drug combinations that fulfill  
274 both the sensitivity and synergy criteria, while avoiding the false positive drug combinations that  
275 might be synergistic but do not achieve a sufficient high level of sensitivity. Taken together, the  
276 combined use of CSS drug combination sensitivity score and its associated synergy score allows a  
277 simultaneous evaluation of the sensitivity and synergy for a drug combination, which will facilitate  
278 a more systematic analysis of high-throughput drug combination data with much less experimental  
279 materials.

280 **Fig. 3. (A) The ROC curves for the CSS-based synergy scores to detect true synergistic and**  
281 **antagonistic drug combinations. (B) The S-S plot for all the drug combinations.** The drug  
282 combinations with the 75<sup>th</sup> percentile and above for both the CSS and the S scores were considered  
283 as the prioritized hits for further experimental validation and highlighted in red.

284

## 285 Discussion

286 Drug combinations may potentially lead to more durable clinical responses by overcoming  
287 intra-tumoral heterogeneity and drug resistance to monotherapies. Identifying drug combinations  
288 that are tailored for personalized medicine is a challenge, as the number of possible combinations  
289 may easily grow exponentially [21]. High-throughput drug combination screening has been  
290 increasingly utilized for early detection of true synergistic and effective drug combinations.  
291 However, systematic identification of drug combinations is difficult, as the concepts of synergistic  
292 versus effective drug combinations are often intertwined and sometimes interchanged without  
293 sufficient clarification. Furthermore, there is a lack of consensus on what the definition of synergy  
294 is, which might contribute to the poor reproducibility of many drug combination studies. The

295 uncertainty about the endpoint measurement in drug combination screens brings additional  
296 complexity for any machine learning approach to tackle the prediction problem.

297 We developed a novel scoring approach called CSS for drug combinations that can be  
298 efficiently determined using a simple experimental design. We found that the CSS is highly replicable  
299 and therefore can be considered as a robust metric to characterize drug combination sensitivity. To  
300 leverage the drug combination CSS data, we also developed a testing platform to allow for a  
301 systematic evaluation of the prediction accuracy of different machine learning methods. We found  
302 that the target information for the compounds as well as their chemical fingerprints are highly  
303 predictive of the CSS values, with an accuracy comparable to the experimental replicates. Therefore,  
304 the rationale of considering a drug combination as a combination of their target and fingerprint  
305 profiles can be justified. This would also allow the augmentation of single-drug screening and drug  
306 combination screening data to train a machine learning model, as many drugs are multi-targeted  
307 which are equivalent to a drug combination with the same target profile. In this study we focused  
308 on drug combination prediction within the same cell line. In the future, we would include the  
309 molecular features of the cell lines to improve the prediction accuracy as well as identify drug  
310 combination specific biomarkers across different cell lines. On the other hand, as the focus of the  
311 current study is to propose the new experimental design and to justify its associated drug  
312 combination scoring methods, we tested the predictability of CSS using conventional machine  
313 learning methods, and showed that CSS can be accurately inferred from the pharmacological  
314 features of drug combinations. More advanced machine learning methods such as Deep Learning  
315 [16] or network-based methods [22] may further improve the prediction accuracy, which will be  
316 tested as future work.

317 A truly promising drug combinations shall reach therapeutic efficacy via a strong synergy.  
318 While there have been multiple synergy scoring methods that can be applied to the full dose-

319 response matrix design, they do not always produce the consistent results. The truly synergistic and  
320 antagonistic drug combinations may therefore be determined by finding the consensus across the  
321 different scoring methods [12]. We developed a CSS-based synergy score to quantify the degree of  
322 interactions in a drug pair, and showed that the CSS-based synergy score can identify the truly  
323 synergistic and antagonistic drug combinations accurately. Therefore, the CSS-based synergy score  
324 can be used for the prioritization of a primary drug combination screen using the cross design, after  
325 which only the significant drug combinations warrant a confirmation screen using the full dose-  
326 response matrix design. Furthermore, we proposed a novel S-S plot to visualize drug combination  
327 sensitivity and synergy using the same scale, which enables an unbiased way to explore high-  
328 throughput drug combination data more efficiently. On the other hand, the CSS is defined at the  
329  $IC_{50}$  concentrations of the background drugs. Therefore, a synergistic drug combination determined  
330 by the CSS-based synergy score should be more therapeutically relevant than a drug combination  
331 where the synergy is detected at a higher concentrations, which are often associated with unwanted  
332 off-target effects and side-effects.

333         The advantage of the proposed cross design is that drug combination screens and single-  
334 drug screens can be implemented in a sequential manner, which requires much less cells and  
335 compound materials compared to a full dose-response matrix. With the introduction of CSS scoring,  
336 we are foreseeing a lower technical barrier to carry out large scale drug combination studies with  
337 minimal cellular materials. Although the drug combination data we explored here involves cancer  
338 cell lines, the cross design and its CSS scoring can be readily applied for ex-vivo drug screening,  
339 where the amount of patient-derived materials can be extremely limited and technically difficult to  
340 obtain due to culture constraints [23]. With the help of CSS and its visualization tools, drug  
341 combination discovery can be more quickly advance and may eventually lead to the validation of  
342 personalized drug combinations in clinical trials.

343

## 344 **Materials and Methods**

### 345 **The cross drug combination design**

346 We proposed a cross design to test the synergy and sensitivity of a drug pair by first  
347 introducing the concepts of background drug and foreground drug: background drug is the drug  
348 fixed at its  $IC_{50}$  concentration while foreground drug is added into the background drug with multiple  
349 concentrations. We allow that either drug in the pair to be the background drug, so that two vectors  
350 of dose mixtures will be produced and intersected at the  $IC_{50}$  concentrations (Fig 4). The dose-  
351 response curves for these two vectors will be determined using cell viability or toxicity assays, where  
352 the inhibition percentages can be calculated using negative and positive controls. Note that the  
353 cross design requires specifically the combinations at the  $IC_{50}$  concentrations, which need to be  
354 determined based on single drug sensitivity screening or prior knowledge.

355 **Fig. 4. The cross design to determine the drug combination sensitivity score.** Compared to the full-  
356 dose response matrix design (left panel), only the single row and single column that correspond to  
357 the  $IC_{50}$  concentrations of the two drugs were utilized for the calculation of CSS (middle panel).  
358 Either Drug1 or Drug2 can be considered as the background drug fixed at its  $IC_{50}$  concentration while  
359 the other is considered as the foreground drug with multiple doses being titrated. The resulting two  
360 dose-response curves will be summarized as the drug combination sensitivity score (CSS), from  
361 which a synergy score can also be calculated as the deviation from the expected value when there  
362 is no interaction.

### 363 **Determination of the CSS drug combination sensitivity scores**

364 With the drug combination dose-response curves determined in the cross design, the CSS  
365 summarizes the area under the curve similar to the AUC and DSS (Drug Sensitivity Score) scoring



366 approaches [24-25]. Namely, a four-parameter log-logistic function is used to fit the dose-response  
367 curve for a concentration  $x$  of the foreground drug according to:

368 
$$y = y_{min} + \frac{y_{max} - y_{min}}{1 + 10^{\lambda(\log_{10} IC_{50} - \log_{10} x)}}, \quad (1)$$

369 where  $y_{min}$  and  $y_{max}$  are the minimal and maximal inhibition (the bottom and top asymptotes of the  
370 curve,  $0 \leq y, y_{min}, y_{max} \leq 1$ ;  $IC_{50}$  is the concentration of the foreground drug with which the drug  
371 combination reaches 50% inhibition of the cell growth;  $\lambda$  is the slope of the dose-response curve.

372 The dose-response curve (1) is transformed by substituting  $x$  with  $x' = \log_{10}(x)$  as:

373 
$$y = y_{min} + \frac{y_{max} - y_{min}}{1 + 10^{\lambda(\log_{10} IC_{50} - x')}} \quad (2)$$

374 The area under the  $\log_{10}$ -scaled dose-response curve (AUC) is determined according to

375 
$$AUC = \int_{c_1}^{c_2} y_{min} + \frac{y_{max} - y_{min}}{1 + 10^{\lambda(m - x')}} dx' = y_{min}(c_2 - c_1) + (y_{max} - y_{min}) \frac{1}{\lambda} \log_{10} \left( \frac{1 + 10^{\lambda(c_2 - m)}}{1 + 10^{\lambda(c_1 - m)}} \right), \quad (3)$$

376 where  $[c_1, c_2]$  is the  $\log_{10}$  concentration range for the foreground drug tested in the experiment, and  
377  $m = \log_{10}(IC_{50})$ .

378 The AUC is further normalized as the proportion of its theoretical upper bound according to:

379 
$$AUC' = \frac{AUC - t(c_2 - c_1)}{(1 - t)(c_2 - c_1)}, \quad (4)$$

380 where  $t$  is the minimum inhibition level that is considered meaningful (by default it is fixed at 10%,  
381 assuming that the inhibition below 10% is experimental noise).

382 The CSS for the foreground drug is defined as a percentage and varies between 0 and 100:

383 
$$CSS = 100AUC' \quad (5)$$

384 As there are two drug combination dose-response curves depending on which drug is fixed  
385 as the background drug, we refer to the results of Eq. (5) for either scenario as  $CSS_1$  and  $CSS_2$ , and  
386 consider them as two samples that are generated from the same random variable. We take the  
387 average of  $CSS_1$  and  $CSS_2$  as the CSS for the drug pair, i.e.

388 
$$CSS = (CSS_1 + CSS_2)/2 \quad (6)$$

389

### 390 **The O'Neil drug combination data**

391 Dose-response was measured as percentage of cell viability and retrieved from the  
392 supplementary material of [17], which includes 22,737 experiments for 583 drug pairs that involves  
393 38 unique drugs in 39 cancer cell lines, representing 7 tissue types. At the first stage, single-drug  
394 screening was done using 8 concentrations to determine the  $IC_{50}$  concentration for each drug with  
395 six replicates. At the second stage, a 4 by 4 dose matrix was utilized to cover the span of  $IC_{50}$   
396 concentrations for a drug pair with four replicates. To utilize the cross design, we picked up only the  
397 row and the column corresponding to the concentrations closest to the  $IC_{50}$  of the single drugs.  
398 These two vectors thus allowed the fitting of drug combination dose-response curves with which  
399 the CSS can be calculated. The cell viability percentage was first transformed to inhibition  
400 percentage according to:

401 
$$\%inhibition = 100 - \%viability \quad (7)$$

402 In our analysis, the average % inhibition of the four replicates was used to calculate the CSS.  
403 The robustness of the CSS values was assessed using the Pearson correlation across the four  
404 replicates.

405

### 406 **Predicting the CSS using machine learning approaches**

407 With the CSS being determined for each drug combination, we sought to evaluate the  
408 prediction accuracy of multiple machine learning methods. We considered a drug combination as a  
409 combination of their targets and chemical fingerprints. We collected the known targets that have  
410 been experimentally validated for the 38 drugs from Drugbank [26] and ChEMBL [27]. Furthermore,  
411 we also utilized the Similarity Ensemble Approach (SEA) to predict additional secondary targets

412 based on the chemical structures of the drugs [28]. The targets that were predicted with Z-score  
413 higher than 20, Tanimoto coefficient higher than 0.4 and P-value smaller than 0.01 were included.  
414 The MACCS fingerprints of the drugs were determined using the SMILES strings with the R package  
415 *rcdk* [29]. The resulting feature set for a drug combination altogether included 398 validated and  
416 predicted targets and 166 MACCS fingerprints (Table S1 and S2).

417 We compared three state-of-the-art machine learning methods for the CSS prediction:  
418 Elastic Net [30], Random Forests [31] and Support Vector Machines [32]. Elastic Net is a  
419 regularization and feature selection method that combines both ridge and lasso regression by  
420 including the  $L_1$  and  $L_2$  penalty terms. This method depends heavily on its penalty term that is  
421 regulated by hyper parameters  $\alpha$  and  $\lambda$ . In our studies,  $\alpha$  was selected from the interval [0.1, 1] and  
422  $\lambda$  was chosen to minimize the difference between predicted and actual CSS scores. Random Forests  
423 is an ensemble learning method that constructs multiple decision trees. In our studies, we set the  
424 number of randomly selected predictors that is used at each split of the decision tree equal to the  
425 rounded down square root of the number of variables. For Support Vector Machines, the tuning  
426 parameters are the cost parameter  $C$  that sets the penalty for misclassification of a training point  
427 and a smoothing parameter  $\sigma$ , based on the accuracy of predictions in cross-validation.

428 We focused on the model performance for predicting new drug combinations within the  
429 same cell line, as the set of drug combinations in the training data did not overlap with that in the  
430 test data. For each cell line, we randomly sampled 70% of the drug combinations to train multiple  
431 machine learning models using 10-fold cross-validation. The optimized models were then used for  
432 predicting the CSS values for the remaining 30% of the novel drug combinations. The same  
433 processes were repeated 20 times by randomly splitting the training and test data. Four metrics  
434 including coefficient of determination ( $R^2$ ), root mean square error (RMSE), mean absolute error  
435 (MAE) and Pearson correlation (COR) were utilized for model comparison. To benchmark the

436 performance of the machine learning methods, we utilized one randomly selected technical  
437 replicate as the prediction to obtain the upper limit of the performance. All the methods were  
438 implemented and evaluated using the R package *caret* [33].

439

#### 440 **Determination of the CSS-based drug synergy scores**

441 The advantage of CSS is that it allows a direct comparison of the sensitivity between a drug  
442 combination and its single drugs, and hence facilitates the quantification of drug synergy. The  
443 degree of synergy is often calculated as the deviation of the observed drug combination effect from  
444 the reference, which is defined as the expectation effect if the drugs are not interacting. We defined  
445 three variants of CSS-based synergy scores (termed as S scores) as:

$$446 \quad S_{\text{sum}} = \text{CSS} - \text{sum}(\text{DSS}_1, \text{DSS}_2), \quad (8)$$

$$447 \quad S_{\text{max}} = \text{CSS} - \text{max}(\text{DSS}_1, \text{DSS}_2), \quad (9)$$

$$448 \quad S_{\text{mean}} = \text{CSS} - \text{mean}(\text{DSS}_1, \text{DSS}_2), \quad (10)$$

449 where the expectation was determined as a summary statistics of the normalized AUC based on the  
450 single drug dose-response curves (termed as DSS values as proposed in [25]). For a non-synergistic  
451 drug pair, the S score is expected to be zero. To evaluate the prediction accuracy of the CSS-based  
452 synergy scores, we defined a set of true synergistic and antagonistic drug combinations as the gold  
453 standard, which were determined using the full dose-response matrix data. We utilized the R  
454 package *synergyfinder* [34] to calculate multiple versions of synergy scores including the HSA  
455 (Highest single agency, [35]), the Bliss [36], the Loewe [37] and the ZIP synergy scores [38]. The  
456 principles of these four models were briefed as below:

457 Consider that drug 1 at concentration  $x_1$  and drug 2 at concentration  $x_2$  were combined to  
458 produce the inhibition effect of  $y_c$ , while their respective single drug effects were  $y_1(x_1)$  and  $y_2(x_2)$ .

459 The synergy score was calculated as the difference between  $y_c$  and the expected effect  $y_e$  if there is  
460 no synergy. Each synergy scoring took a different model for  $y_e$ :

461 1. HSA:  $y_e$  is the maximal single drug effect, defining

$$462 \quad S_{\text{HSA}} = y_c - \max(y_1(x_1), y_2(x_2)) \quad (11)$$

463 2. Bliss:  $y_e$  is the expected effect of two drugs acting independently, defining

$$464 \quad S_{\text{Bliss}} = y_c - (y_1(x_1) + y_2(x_2) - y_1(x_1)y_2(x_2)) \quad (12)$$

465 3. Loewe:  $y_e$  is the expected effect of a drug combined with itself, defining

$$466 \quad S_{\text{Loewe}} = y_c - y_1(x_1 + x_2) = y_c - y_2(x_1 + x_2) \quad (13)$$

467 4. ZIP:  $y_e$  is the expected effect of two drugs that do not potentiate each other, defining

$$468 \quad S_{\text{ZIP}} = y_c' - (y_1'(x_1) + y_2'(x_2) - y_1'(x_1)y_2'(x_2)), \quad (14)$$

469 where  $y_c', y_1'(x_1)$  and  $y_2'(x_2)$  are the fitted values based on the full-dose response matrix for the  
470 combination and single drugs, respectively.

471 For each of the four models, the synergy scores were determined first for a given dose  
472 combination and then were averaged over the full dose-response matrix. With the four synergy  
473 scores determined for each drug combination, the true synergistic and antagonistic drug  
474 combinations are those with all the four synergy scores consistently higher than 5 and lower than  
475 5, respectively. The aim was then to use the CSS-based synergy score which was determined by the  
476 cross design data to predict the ground truth determined by the full dose-response matrix design.  
477 The area under the ROC curve was used for evaluating how well the CSS-based synergy scores can  
478 predict the consensus drug combinations determined using the full dose-response matrix data.

479

## 480 **Acknowledgements**

481 This work was supported by the European Research Council Starting Grant agreement No  
482 716063 (DrugComb), Academy of Finland Grant agreement No. 317689 and Helsinki Institute of Life

483 Sciences Research Fellow funding. A.M and W.W. are supported by the FIMM-EMBL PhD program  
484 scholarship. We thank the authors of the O'Neil study for making the drug combination data fully  
485 accessible.

486

## 487 **References**

- 488 1. Lawrence MS, Stojanov P, Mermel CH, Robinson JT, Garraway LA, Golub TR, Meyerson M, Gabriel  
489 SB, Lander ES, Getz G. Discovery and saturation analysis of cancer genes across 21 tumour types.  
490 Nature. 2014;505(7484):495.
- 491 2. Hanahan D. Rethinking the war on cancer. The Lancet. 2014;383(9916):558-563.
- 492 3. Crystal AS, Shaw AT, Sequist LV, Friboulet L, Niederst MJ, Lockerman EL, Frias RL, Gainor JF,  
493 Amzallag A, Greninger P, Lee D. Patient-derived models of acquired resistance can identify effective  
494 drug combinations for cancer. Science. 2014;346(6216):1480-1486.
- 495 4. Dry JR, Yang M, Saez-Rodriguez J. Looking beyond the cancer cell for effective drug combinations.  
496 Genome Medicine. 2016;8(1):125.
- 497 5. Held MA, Langdon CG, Platt JT, Graham-Steed T, Liu Z, Chakraborty A, Bacchiocchi A, Koo A,  
498 Haskins JW, Bosenberg MW, Stern DF. Genotype-selective combination therapies for melanoma  
499 identified by high-throughput drug screening. Cancer Discovery. 2013;3(1):52-67.
- 500 6. Gianni M, Qin Y, Wenes G, Bandstra B, Conley AP, Subbiah V, Leibowitz-Amit R, Ekmekcioglu S,  
501 Grimm EA, Roszik J. High-throughput architecture for discovering combination cancer therapeutics.  
502 JCO Clinical Cancer Informatics. 2018;11;2:1-2.
- 503 7. Al-Lazikani B, Banerji U, Workman P. Combinatorial drug therapy for cancer in the post-genomic  
504 era. Nature Biotechnology. 2012;30(7):679-692.
- 505 8. Gottesman MM, Lavi O, Hall MD, Gillet JP. Toward a better understanding of the complexity of  
506 cancer drug resistance. Annual Review of Pharmacology and Toxicology. 2016;56:85-102.

- 507 9. Doroshow JH, Simon RM. On the design of combination cancer therapy. *Cell*. 2017;171(7):1476-  
508 1478.
- 509 10. Griner LA, Guha R, Shinn P, Young RM, Keller JM, Liu D, Goldlust IS, Yasgar A, McKnight C, Boxer  
510 MB, Duvéau DY. High-throughput combinatorial screening identifies drugs that cooperate with  
511 ibrutinib to kill activated B-cell–like diffuse large B-cell lymphoma cells. *Proceedings of the National  
512 Academy of Sciences*. 2014;111(6):2349-2354.
- 513 11. Licciardello MP, Ringler A, Markt P, Klepsch F, Lardeau CH, Sdelci S, Schirghuber E, Müller AC,  
514 Caldera M, Wagner A, Herzog R. A combinatorial screen of the CLOUD uncovers a synergy targeting  
515 the androgen receptor. *Nature Chemical Biology*. 2017;13(7):771-778.
- 516 12. Tang J, Wennerberg K, Aittokallio T. What is synergy? The Saariselkä agreement revisited.  
517 *Frontiers in Pharmacology*. 2015;6:181.
- 518 13. Haverty PM, Lin E, Tan J, Yu Y, Lam B, Lianoglou S, Neve RM, Martin S, Settleman J, Yauch RL,  
519 Bourgon R. Reproducible pharmacogenomic profiling of cancer cell line panels. *Nature*.  
520 2016;533(7603):333-337.
- 521 14. Palmer AC, Sorger PK. Combination cancer therapy can confer benefit via patient-to-patient  
522 variability without drug additivity or synergy. *Cell*. 2017;171(7):1678-1691.
- 523 15. Smirnov P, Kofia V, Maru A, Freeman M, Ho C, El-Hachem N, Adam GA, Ba-alawi W, Safikhani Z,  
524 Haibe-Kains B. PharmacODB: an integrative database for mining in vitro anticancer drug screening  
525 studies. *Nucleic Acids Research*. 2017;46(D1):D994-1002.
- 526 16. Preuer K, Lewis RP, Hochreiter S, Bender A, Bulusu KC, Klambauer G. DeepSynergy: predicting  
527 anti-cancer drug synergy with Deep Learning. *Bioinformatics*. 2017;34(9):1538-1546.
- 528 17. O'Neil J, Benita Y, Feldman I, Chenard M, Roberts B, Liu Y, Li J, Kral A, Lejnine S, Loboda A, Arthur  
529 W. An unbiased oncology compound screen to identify novel combination strategies. *Molecular  
530 Cancer Therapeutics*. 2016;15(6):1155-1162.

- 531 18. Durant JL, Leland BA, Henry DR, Nourse JG. Reoptimization of MDL keys for use in drug discovery.  
532 *Journal of Chemical Information and Computer Sciences*. 2002;42(6):1273-1280.
- 533 19. Pommier Y, Leo E, Zhang H, Marchand C. DNA topoisomerases and their poisoning by anticancer  
534 and antibacterial drugs. *Chemistry & Biology*. 2010;17(5):421-433.
- 535 20. Bianchini G, Balko JM, Mayer IA, Sanders ME, Gianni L. Triple-negative breast cancer: challenges  
536 and opportunities of a heterogeneous disease. *Nature Reviews Clinical Oncology*. 2016;13(11):674.
- 537 21. Iorio F, Knijnenburg TA, Vis DJ, Bignell GR, Menden MP, Schubert M, Aben N, Gonçalves E,  
538 Barthorpe S, Lightfoot H, Cokelaer T. A landscape of pharmacogenomic interactions in cancer. *Cell*.  
539 2016;166(3):740-754.
- 540 22. Li H, Li T, Quang D, Guan Y. Network propagation predicts drug synergy in cancers. *Cancer*  
541 *Research*. 2018;78(18):5446-5457.
- 542 23. Letai A. Functional precision cancer medicine—moving beyond pure genomics. *Nature*  
543 *Medicine*. 2017;23(9):1028-1035.
- 544 24. Yang W, Soares J, Greninger P, Edelman EJ, Lightfoot H, Forbes S, Bindal N, Beare D, Smith JA,  
545 Thompson IR, Ramaswamy S. Genomics of Drug Sensitivity in Cancer (GDSC): a resource for  
546 therapeutic biomarker discovery in cancer cells. *Nucleic Acids Research*. 2012;41(D1):D955-961.
- 547 25. Yadav B, Pemovska T, Sz wajda A, Kuleskiy E, Kontro M, Karjalainen R, Majumder MM, Malani  
548 D, Murumägi A, Knowles J, Porkka K. Quantitative scoring of differential drug sensitivity for  
549 individually optimized anticancer therapies. *Scientific Reports*. 2014;4:5193.
- 550 26. Wishart DS, Feunang YD, Guo AC, Lo EJ, Marcu A, Grant JR, Sajed T, Johnson D, Li C, Sayeeda Z,  
551 Assempour N. DrugBank 5.0: a major update to the DrugBank database for 2018. *Nucleic Acids*  
552 *Research*. 2017;46(D1):D1074-1082.



- 553 27. Gaulton A, Hersey A, Nowotka M, Bento AP, Chambers J, Mendez D, Motowolo P, Atkinson F, Bellis  
554 LJ, Cibrián-Uhalte E, Davies M. The ChEMBL database in 2017. *Nucleic Acids Research*.  
555 2016;45(D1):D945-954.
- 556 28. Keiser MJ, Roth BL, Armbruster BN, Ernsberger P, Irwin JJ, Shoichet BK. Relating protein  
557 pharmacology by ligand chemistry. *Nature Biotechnology*. 2007;25(2):197-206.
- 558 29. Guha R. Chemical informatics functionality in R. *Journal of Statistical Software*. 2007;18(5):1-6.
- 559 30. Zou H, Hastie T. Regularization and variable selection via the elastic net. *Journal of the Royal*  
560 *Statistical Society: Series B (Statistical Methodology)*. 2005;67(2):301-320.
- 561 31. Breiman L. Random forests. *Machine Learning*. 2001;45(1):5-32.
- 562 32. Ben-Hur A, Ong CS, Sonnenburg S, Schölkopf B, Rätsch G. Support vector machines and kernels  
563 for computational biology. *PLoS Computational Biology*. 2008;4(10):e1000173.
- 564 33. Kuhn M. Caret package. *Journal of Statistical Software*. 2008;28(5):1-26.
- 565 34. He L, Kuleskiy E, Saarela J, Turunen L, Wennerberg K, Aittokallio T, Tang J. Methods for high-  
566 throughput drug combination screening and synergy scoring. *Methods in Molecular Biology*.  
567 2018;1711:351-398.
- 568 35. Berenbaum, MC. What is synergy? *Pharmacological Review*. 1989;41(2):93-141.
- 569 36. Bliss CI. The toxicity of poisons applied jointly. *Annals of Applied Biology*. 1939;26(3):585-615.
- 570 37. Loewe S. The problem of synergism and antagonism of combined drugs. *Arzneimittelforschung*.  
571 1953;3(6):285-290.
- 572 38. Yadav B, Wennerberg K, Aittokallio T, Tang J. Searching for drug synergy in complex dose-  
573 response landscapes using an interaction potency model. *Computational and structural*  
574 *biotechnology journal*. 2015;13:504-513.
- 575

576 **Supporting Information**

577 Table S1. Drug target profiles including experimentally-validated primary and secondary targets, and

578 SEA-predicted secondary targets for the 38 compounds [SupTable1.xlsx]

579 Table S2. The chemical information including MACCS fingerprint profiles for the 38 compounds

580 [SupTable2.xlsx]

581 Table S3. The correlations of the CSS values obtained using the average of four viability replicates,

582 with the CSS values obtained from the replicate separately [SupTable3.xlsx].

583 Table S4. CSS drug combination sensitivity scores and S synergy scores for each drug combination

584 [SupTable4.xlsx]

585 Fig S1. The heatmap of the CSS1-CSS2 correlations sorted by drug combinations. Drug classes are

586 shown in different colors at the edges of the heatmap.

587 Fig S2. Replicability of CSS values over the replicates. The line plot of the minimal and maximal values

588 for the CSS replicates combined with CSS values over the standard deviation of the CSS replicates.

589 Fig S3. The coefficient of variation (CV) for each drug in the single drug screens. The correlations

590 between CSS1 and CSS2 for the drug combinations that involve a given drug were shown on top of

591 each bar.

592 Fig S4. The correlation between the variable importance of TOP1MT and the average CSS for

593 TOP1MT inhibitor for all the 39 cell lines. LNCAP is the only line which has a negative variable

594 importance for TOP1MT.

$$CSS = (CSS_1 + CSS_2) / 2$$
$$\text{Synergy} = CSS - \text{reference}$$

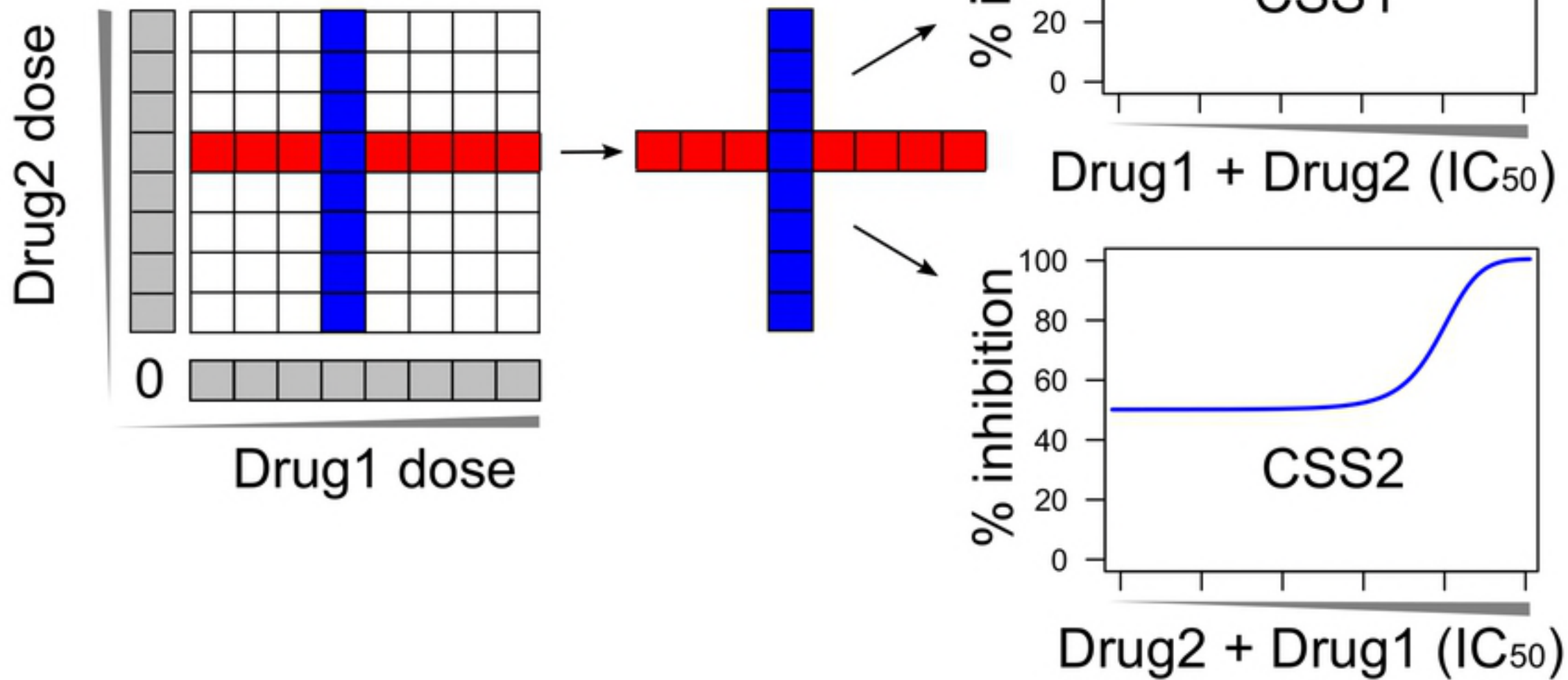


Fig1

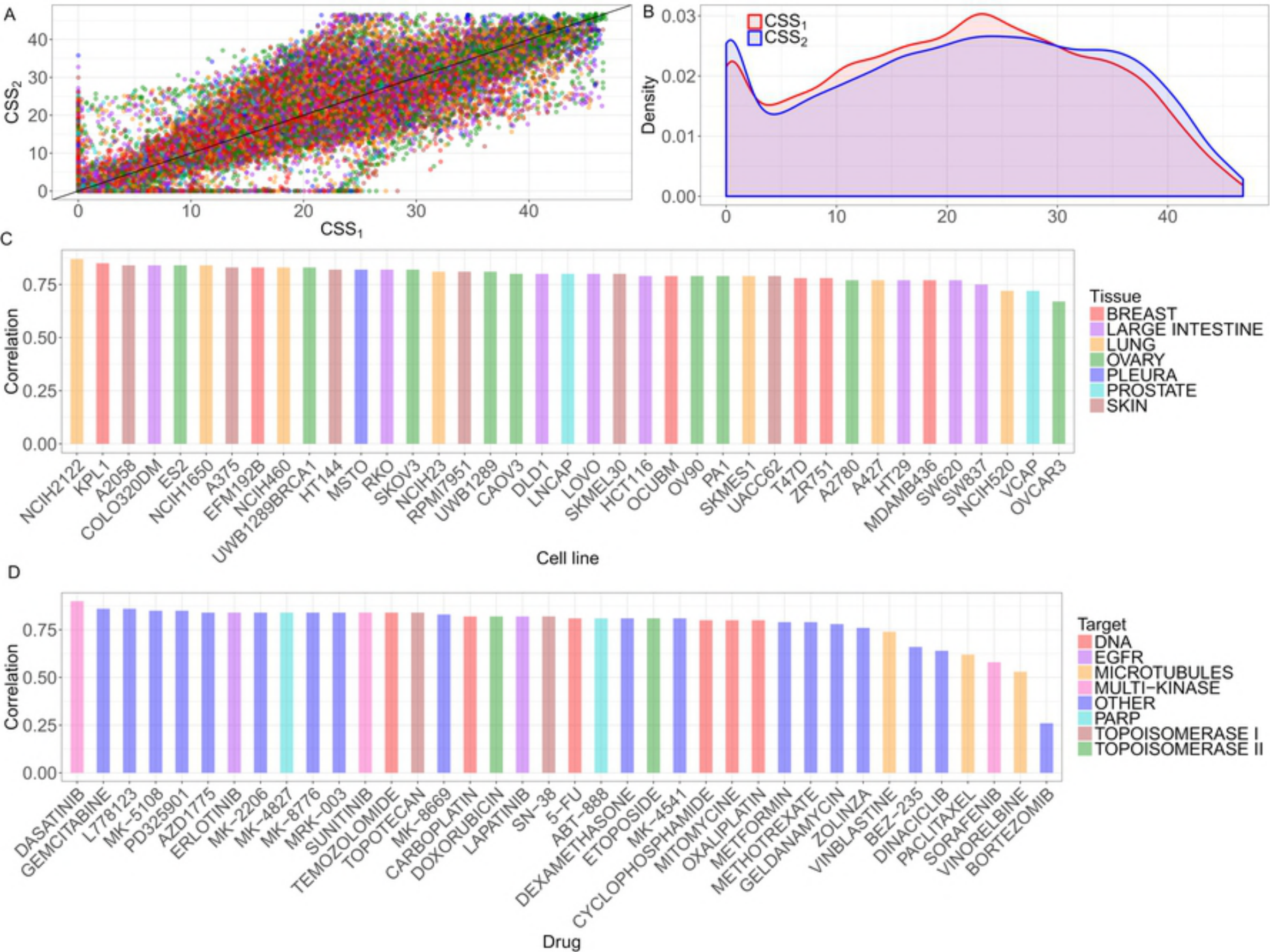


Fig2





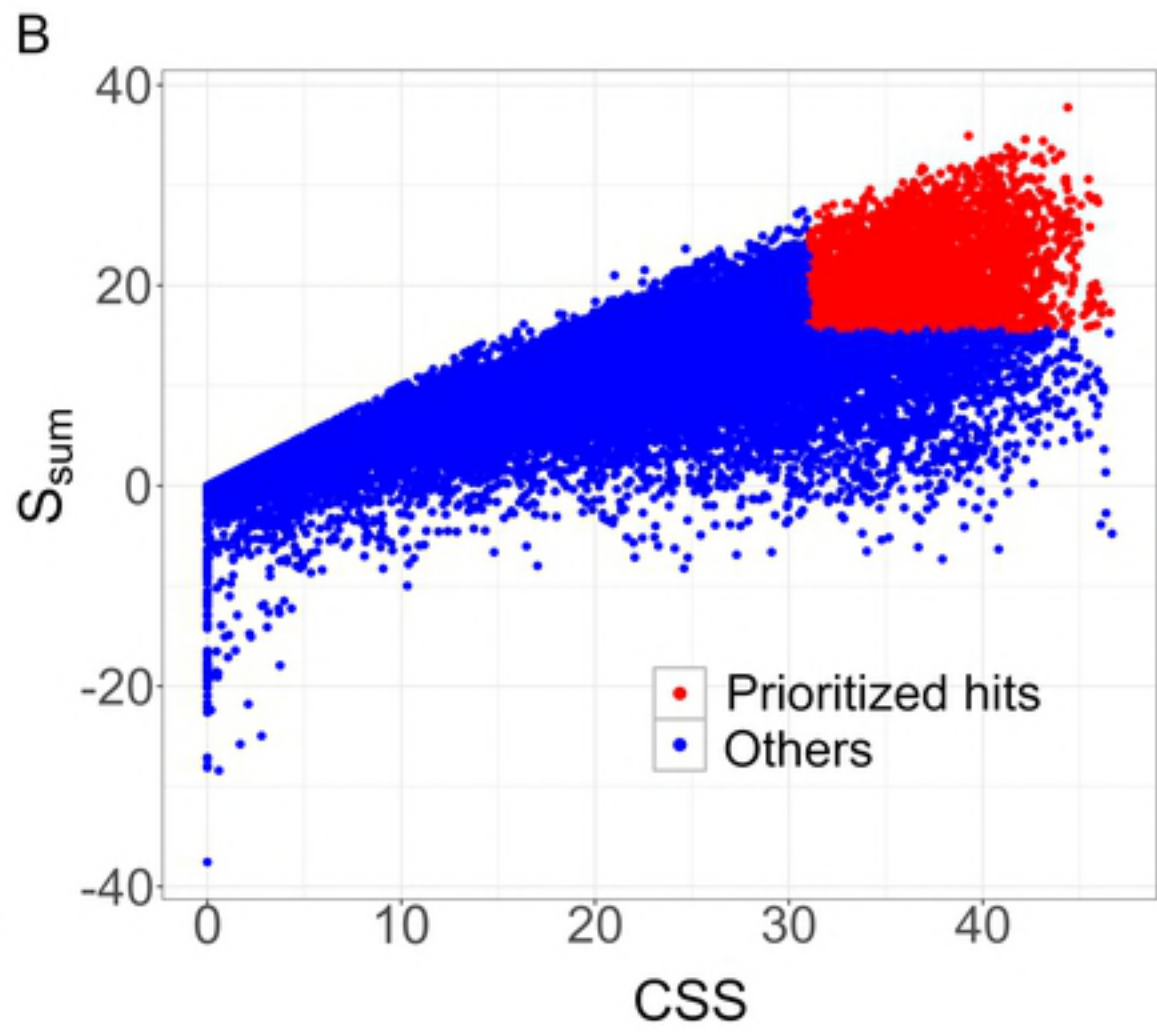
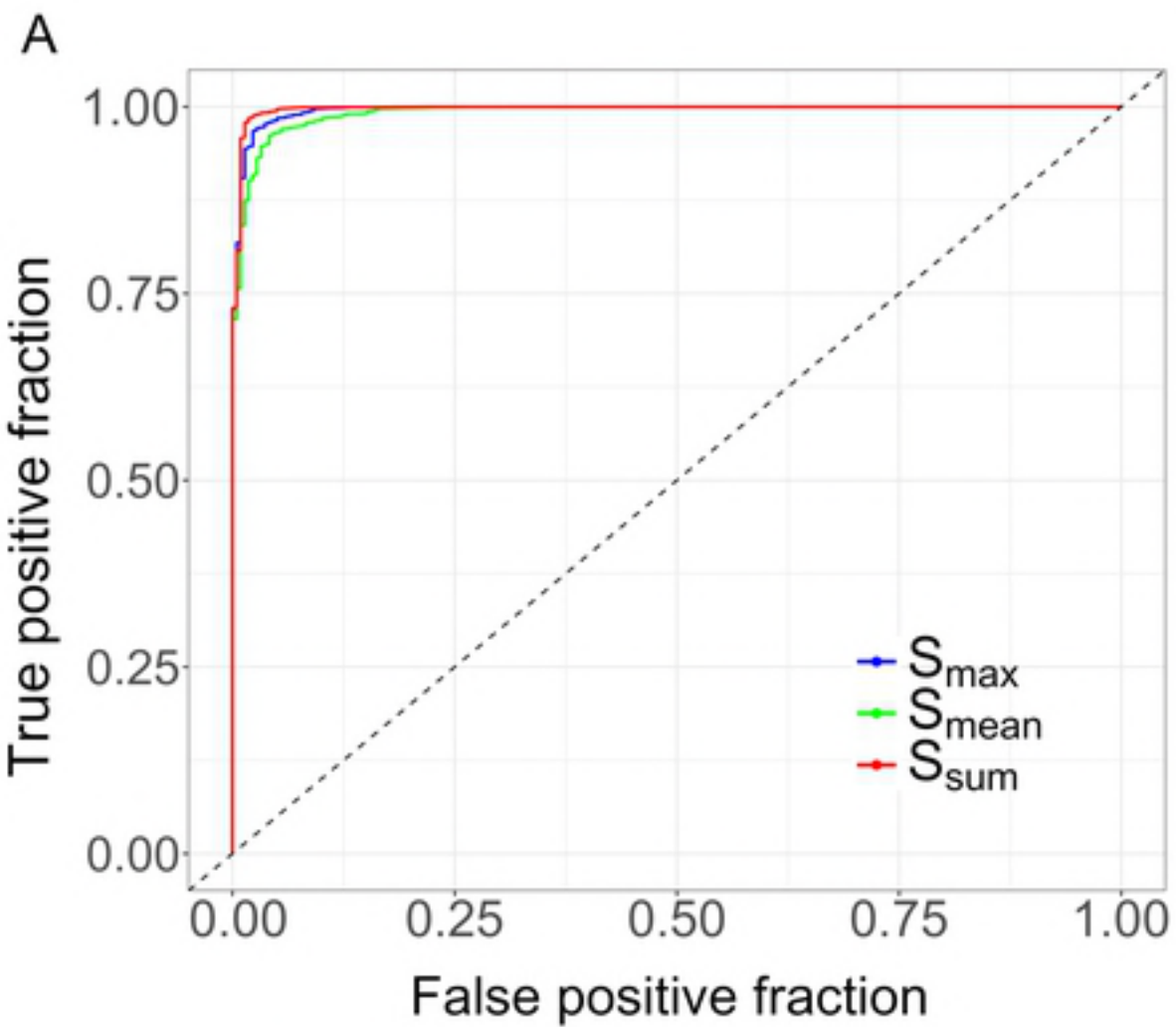


Fig4